DALTON

Applications of extended X-ray absorption fine structure spectroscopy to the study of polyoxometalates †

John Evans,* Martyn Pillinger and Jacqueline M. Rummey

Department of Chemistry, University of Southampton, Southampton SO17 1BJ, UK

Extended X-ray absorption fine structure (EXAFS) spectroscopy has been used to characterise polyoxometalates of the type $M_mO_y^{n-}$ and $X_xM_mO_y^{n-}$ in the solid state and in solution. The best fit to the low-temperature (80 K) niobium K-edge EXAFS of $K_7[HNb_6O_{19}]\cdot 13H_2O$ was obtained with one terminal oxygen at 1.79 Å ($M–O_t$), four doubly bridging oxygens at 1.97 Å ($M–O_b$), four niobiums at 3.32 Å and one niobium at 4.76 Å. The $Nb–O_b–Nb$ bond angle was determined as 113° following a multiple-scattering calculation for this unit. Analysis of the niobium K- and tungsten L_{III}-edge EXAFS of salts of $Nb_xW_{6-x}O_{19}^{(x+2)-}$ (x = 2–4) yielded Nb–O bond lengths of 1.74–1.76 and 1.98–1.99 Å, W–O bond lengths of 1.72–1.74 and 1.89–1.91 Å, and non-bonded M • • • M distances of 3.31–3.35 and 4.74–4.78 Å. The first co-ordination spheres also comprise one six-fold bridging oxygen at about 2.3 Å but this shell is poorly defined due to static and thermal disorder in the bond. A combination of vanadium K- and tungsten L_{III}-edge EXAFS of $[V_2W_4O_{19}]^{4-}$ yielded W • • • W separations of 3.27 Å but shorter V • • • W separations of 3.20 Å, showing a slight distortion in the hexametalate structure that is not observed for the niobotungstates. Molybdenum K-edge EXAFS analysis of $[NBu^n_4]_3[PMo_{12}O_{40}]$ in the solid state at 80 K revealed systematic asymmetry in the $Mo–O_b$ bonds with two oxygens at 1.81 and two at 1.97 Å. The structure is not perturbed when the salt is dissolved in acetonitrile. Likewise the molybdenum K-edge EXAFS of $[TeMo_6O_{24}]^{6-}$ in water and $[Mo_6O_{19}]^{2-}$ in acetonitrile analysed for the same co-ordination spheres as those of the parent salts $Na_3[TeMo_6O_{24}]\cdot nH_2O$ and $[NBu^n_4]_2[Mo_6O_{19}]$.

The early transition-metal polyoxoanions constitute a very large class of discrete, soluble metal oxide-like analogues.[1] They may be represented by the general formulae $M_mO_y^{n-}$ (isopolyanions) and $X_xM_mO_y^{n-}$ (heteropolyanions) where M is usually W^{VI} or Mo^{VI}, less frequently $V^{IV/V}$, Nb^V or Ta^V, or mixtures of these elements. There are few restrictions on the heteroatom (X) and more than 70 elements, both metal and non-metal, are known to exist in heteropolyanions. Water is the preferred solvent for synthesis but non-aqueous methods have also been developed. The rapid structural equilibria that often exist in solution are complex and twenty years ago little was known about the relationships between a crystallised species and those actually existing in solution. Since then X-ray crystallography has yielded hundreds of solid-state structures, ranging in complexity from relatively simple species such as $[V_2O_7]^{4-}$ to large clusters such as $[NaP_5W_{30}O_{110}]^{14-}$. Solution structures can now be characterised in some detail by techniques such as one- and two-dimensional metal and ^{17}O NMR spectroscopies,[2,3] precise electrochemical measurements[4] and Raman spectroscopy.[5]

Our interest in polyoxometalates stems from their use as pillaring agents for layered double hydroxides.[6] Previous studies have shown that chromium K-edge X-ray absorption spectroscopy (XAS) was useful in characterising the species present in chromia pillared smectite clays.[7] We were therefore led to delineate the scope and limitations of XAS as a structural probe in polyoxometalate chemistry. This paper presents and discusses EXAFS (extended X-ray absorption fine structure) analysis data for hexametalates of the type $M_6O_{19}^{n-}$, the decametalates $[W_{10}O_{32}]^{4-}$ and $[V_{10}O_{28}]^{6-}$, the molybdates $[Mo_7O_{24}]^{6-}$, α- and β-$[Mo_8O_{26}^{4-}]$, and heteropolymetalates of the type $[PM_{12}O_{40}]^{3-}$ and $[TeMo_6O_{24}]^{6-}$. Previous studies in this area are due essentially to Watanabe and co-workers[8] who carried out EXAFS experiments on various polyoxomolybdate and -tungstate compounds. Their interpretation of the data and corresponding Fourier transforms was, however, limited to qualitative treatments and comparisons of simulated with experimental spectra.

† *Non-SI unit employed:* eV ≈ 1.60 × 10^{-19} J.

Results and Discussion

X-Ray absorption spectra were recorded for a series of polyoxometalate compounds in solution and/or in the solid state. Data were collected typically out to k = 18 $Å^{-1}$ beyond the absorption edge. No smoothing or Fourier filtering was applied and the fits discussed below are all compared with the raw (background subtracted) EXAFS data. Each shell was added stepwise (the oxygen shells first followed by the more distant M • • • M shells), iterated in the usual way, and the best fits tested for statistical significance. The theoretical curves shown in the figures are those for the models detailed in the tables. The co-ordination numbers have generally been fixed at values predicted from the known structures and configurations of the anions.

Hexametalates

The hexametalate structure was first discovered by Lindqvist[9] in an X-ray investigation of the hexaniobate anion in crystals of $Na_7[HNb_6O_{19}]\cdot 15H_2O$ [Fig. 1(*a*)]. Each metal is co-ordinated by six oxygen atoms [1 ONb terminal (O_t), 4 ONb_2 doubly bridging (O_b) and 1 ONb_6 six-fold bridging (O_c)] in a distorted-octahedral arrangement, the distortion consisting of a displacement of the metal towards O_t. The six NbO_6 octahedra condense so that they all share a common vertex, O_c.

$[HNb_6O_{19}]^{7-}$. Lindqvist[9] found Nb • • • Nb distances of between 3.2 and 3.6 Å in the hexaniobate anion but was unable to determine the oxygen positions. The complete structure of the sodium salt $Na_7[H_3O][Nb_6O_{19}]\cdot 14H_2O$ was later determined by Goiffon *et al.*[13] and Table 1 lists the Nb–O bond lengths and Nb • • • Nb distances found.

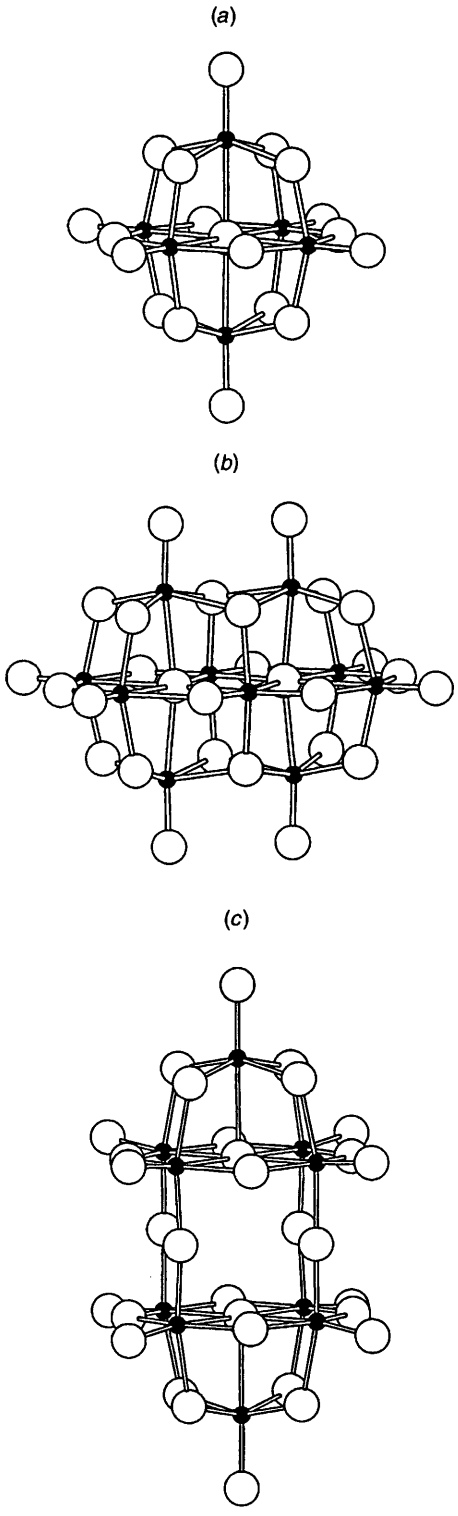

Fig. 1 Bond structures of $M_6O_{19}^{n-}$ (*a*), $[V_{10}O_{28}]^{6-}$ (*b*) and $[W_{10}O_{32}]^{4-}$ (*c*) anions. Large open circles represent oxygen atoms and small filled circles metal atoms. Atomic coordinates from ref. 10 for $[NBu^n_4]_2[Mo_6O_{19}]$, ref. 11 for $K_2Zn_2[V_{10}O_{28}]\cdot 16H_2O$ and ref. 12 for $[NBu^n_3H]_4[W_{10}O_{32}]$

The low-temperature (80 K) niobium K-edge EXAFS of solid $K_7[HNb_6O_{19}]\cdot nH_2O$ was initially fitted by a four-shell model comprising one oxygen atom at 1.79 and four at 1.97 Å, four niobium atoms at 3.32 and one at 4.76 Å (Fig. 2, Table 1). These distances equate with the single-crystal X-ray data for the sodium salt.[13] The interstitial oxygen shell expected at about 2.4 Å was poorly defined (high Debye–Waller factor and high statistical errors) and could not be included in the model. This was found to be the case with many of the spectra analysed in

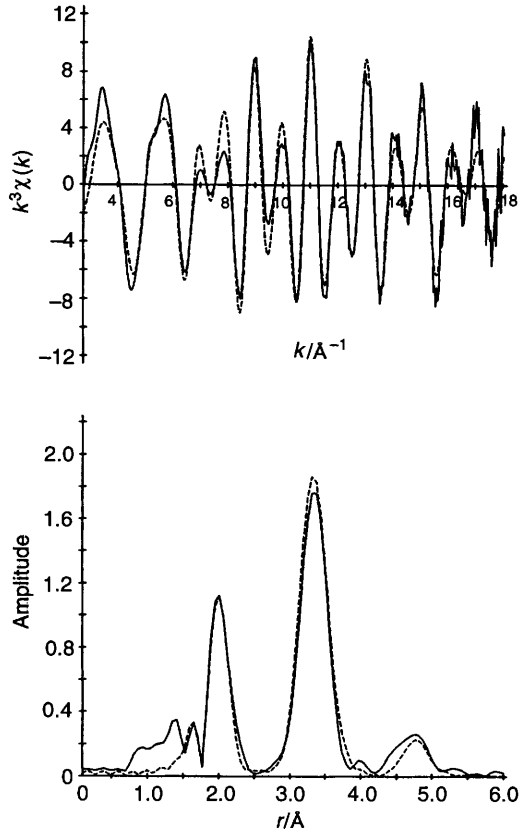

Fig. 2 Niobium K-edge k^3-weighted EXAFS spectrum and Fourier transform, phase-shift corrected for oxygen (——, experimental; – – –, spherical wave theory), of $K_7[HNb_6O_{19}]$ in the solid state at 80 K

this work and is explained by the high thermal and static disorder in the Nb–O_c bond (O_c = three-, four- or six-fold bridging oxygen). The fit to the EXAFS was improved somewhat by allowing multiple scattering for the Nb–O_b–Nb unit. Despite the obtuse Nb–O_b–Nb angle of 115° (calculated from EXAFS-derived distances), a 9% decrease in the fit index (*F*) from 0.33 to 0.30 was observed, with little or no change in the other structural parameters. This angle iterated to a final value of 113° ($F = 0.29$) upon inclusion in the least-squares refinement routine. Using a plane-wave multiple-scattering formalism, Teo[15] showed that such bond-angle determination to an accuracy of 5° was possible even with angles as low as 113°.

$[Mo_6O_{19}]^{2-}$. The k^3-weighted molybdenum K-edge EXAFS of $[NBu^n_4]_2[Mo_6O_{19}]$ in the solid state and in acetonitrile were fitted by four-shell models as for the hexaniobate anion (Fig. 3, Table 1). No direct structural evidence is found for the presence of species other than $[Mo_6O_{19}]^{2-}$ in solution. Inclusion of multiple scattering for the Mo–O_b–Mo units was again beneficial. With a bond angle of 117° (calculated from the mean crystallographic distances), minima with $R = 29.4$ and 26.0% were obtained for the fits to the solid and solution spectra respectively. In both cases the angle refined to 113°. Of particular interest are the unusually high Debye–Waller parameters determined for the shells of four OMo_2 oxygens at 1.87–1.88 Å ($2\sigma^2 = 0.016$–0.018 compared to 0.006–0.009 $Å^2$ for the other hexametalates). The same diminished relative intensity in the Fourier-transform peak for this shell was observed by Miyanaga *et al.*[8] in EXAFS experiments on the same compound. They conclude that the vibrational peak shapes in the Raman spectrum are evidence of high vibrational disorder rather than static disorder in the Mo–O_b bond. This is reasonable given that the crystallographic

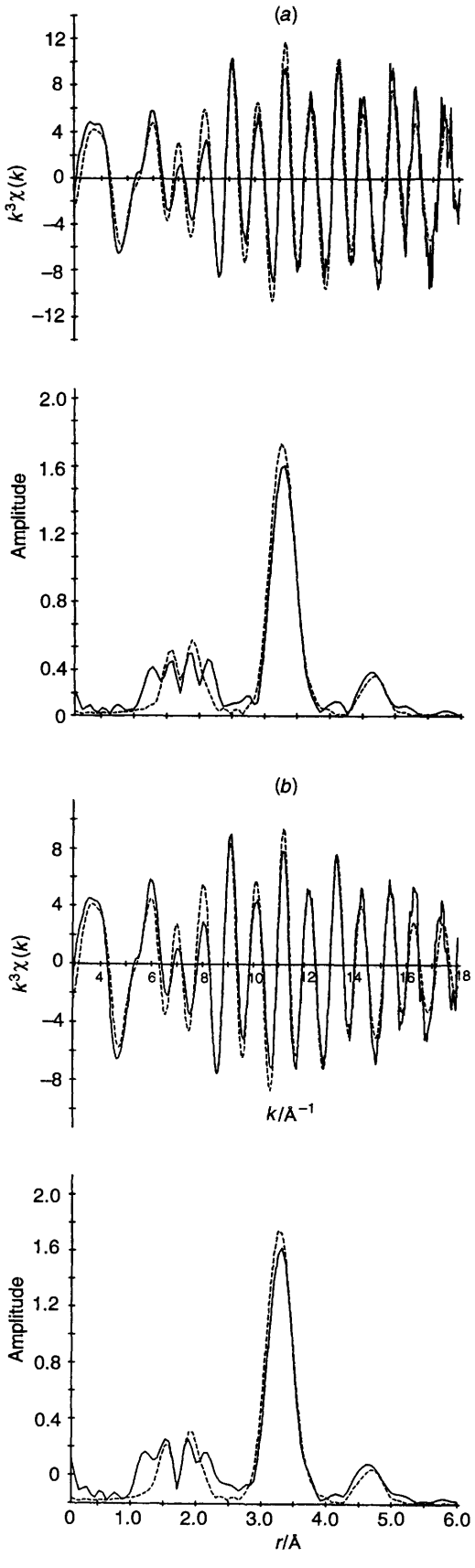

Fig. 3 Molybdenum K-edge k^3-weighted EXAFS spectrum and Fourier transform of $[NBu^n_4]_2[Mo_6O_{19}]$ in the solid state at 80 K (*a*) and in acetonitrile at 25 °C (*b*). Details as in Fig. 2

bond lengths for the tetrabutylammonium salt fall within a relatively narrow range (1.904–1.943 Å) and no systematic asymmetry is identified.[10]

$[VW_5O_{19}]^{3-}$ and $[V_2W_4O_{19}]^{4-}$. A single-crystal X-ray study of the tungstovanadate anion in $[CN_3H_6]_4[V_2W_4O_{19}]$ showed that it has the hexaniobate-type structure but could not ascertain the configuration of the anion because orientational disorder rendered all of the metal atoms equivalent.[14] The crystallographic distances are therefore averaged values of V–O and W–O or V···V, V···W and W···W distances. A large distribution in the M···M separations (3.17–3.35 Å) indicates that the M_6 octahedra are slightly deformed. Subsequent ^{17}O NMR studies have confirmed that in fact only the *cis* isomer is formed.[2]

The tungsten L_{III}-edge EXAFS of solid $Na_4[V_2W_4O_{19}]\cdot nH_2O$ at 80 K was initially modelled by four shells with co-ordination numbers fixed according to the *cis* configuration (Table 1). The well defined W···W distance of 3.27 Å lies just outside the range found in $[W_6O_{19}]^{2-}$ in crystals of $[NBu^n_4]_2[W_6O_{19}]$ (3.281–3.296 Å)[16] and is the same as the equivalent EXAFS-derived distance found in this work for $[W_{10}O_{32}]^{4-}$ in $[NBu^n_4]_4[W_{10}O_{32}]$. The vanadium shell had less than 1% probability of being insignificant according to the Joyner test[17] and brought the fit index from 0.63 to 0.52. Although this W···V distance (3.179 Å) might seem rather short, it still lies within the crystallographic range for M···M. A hexavanadate core with a V···V internuclear distance of about 3.18 Å has been structurally characterised in crystals of $[Rh(\eta\text{-}C_5Me_5)]_4[V_6O_{19}]$.[18] Thus, the EXAFS-derived distance of 3.20 Å in $[V_2W_4O_{19}]^{4-}$ is not unreasonable and may account for the deformation of the M_6 octahedron. A moderate improvement in the model (*R* down to 28.2%) was obtained by fitting one OM_6 oxygen atom at 2.205(15) Å [$2\sigma^2$ = 0.0116(33) Å^2] and one tungsten at 4.627(5) Å [$2\sigma^2$ = 0.0058(7) Å^2]. The V···W distance was verified to some extent by analysis of the vanadium K-edge X-ray absorption spectrum. Despite only having data of poor quality out to k = 12 Å^{-1}, three tungstens were modelled at 3.22 Å in addition to four OM_2 oxygens at 1.91 Å.

In the fit to the room-temperature tungsten L_{III}-edge EXAFS of $[NBu^n_4]_3[VW_5O_{19}]$ no vanadium atom could be reliably modelled at *ca.* 3.2 Å but an acceptable fit was obtained with one tungsten atom at 4.66 Å (Table 1).

$[Nb_xW_{6-x}O_{19}]^{(x+2)-}$ (x = 2–4). An IR and Raman spectroscopic study of these anions in aqueous solution and in the solid state showed that $[Nb_2W_4O_{19}]^{4-}$ and $[Nb_4W_2O_{19}]^{6-}$ are both *cis* isomers (C_{2v} symmetry) while $[Nb_3W_3O_{19}]^{5-}$ is probably a *fac* isomer (C_{3v} symmetry).[5] For each of the niobotungstate anions there is good consistency between the tungsten L_{III}-edge and niobium K-edge EXAFS-derived W···Nb distances (Table 1). The effect of tungsten substitution can be seen in the changing relative intensities of the niobium K-edge Fourier-transform peaks between 2.7 and 4 Å (Fig. 4). Tungsten L_{III}-edge X-ray absorption spectra were recorded at room temperature and at 80 K for $[NMe_4]Na_2K[Nb_2W_4O_{19}]$. Cooling the sample resulted in substantially enhanced EXAFS amplitude towards high k with a concomitant decrease (*ca.* 50%) in the Debye–Waller parameters determined for the M···M shells at 3.3 Å. The EXAFS analysis data for all three anions justify the expected W:Nb ratios and configurations, although one can be less certain about the latter due to high correlations (> 0.8) between the structural parameters of the near tungsten and niobium backscattering shells. These high correlations are not unexpected given the proximity of the two shells and it may be that the accuracy of some of the parameters is less than that normally achievable by EXAFS.

All of the Fourier-transform spectra contain a feature between 4.5 and 5.0 Å corresponding to the long M···M relationship. However, this shell could only be modelled reliably for $[Nb_2W_4O_{19}]^{4-}$ (**Nb**···W 4.74 Å), $[Nb_3W_3O_{19}]^{5-}$ (**W**···Nb 4.78 Å) and $[Nb_4W_2O_{19}]^{6-}$ (**W**···Nb 4.74 Å)

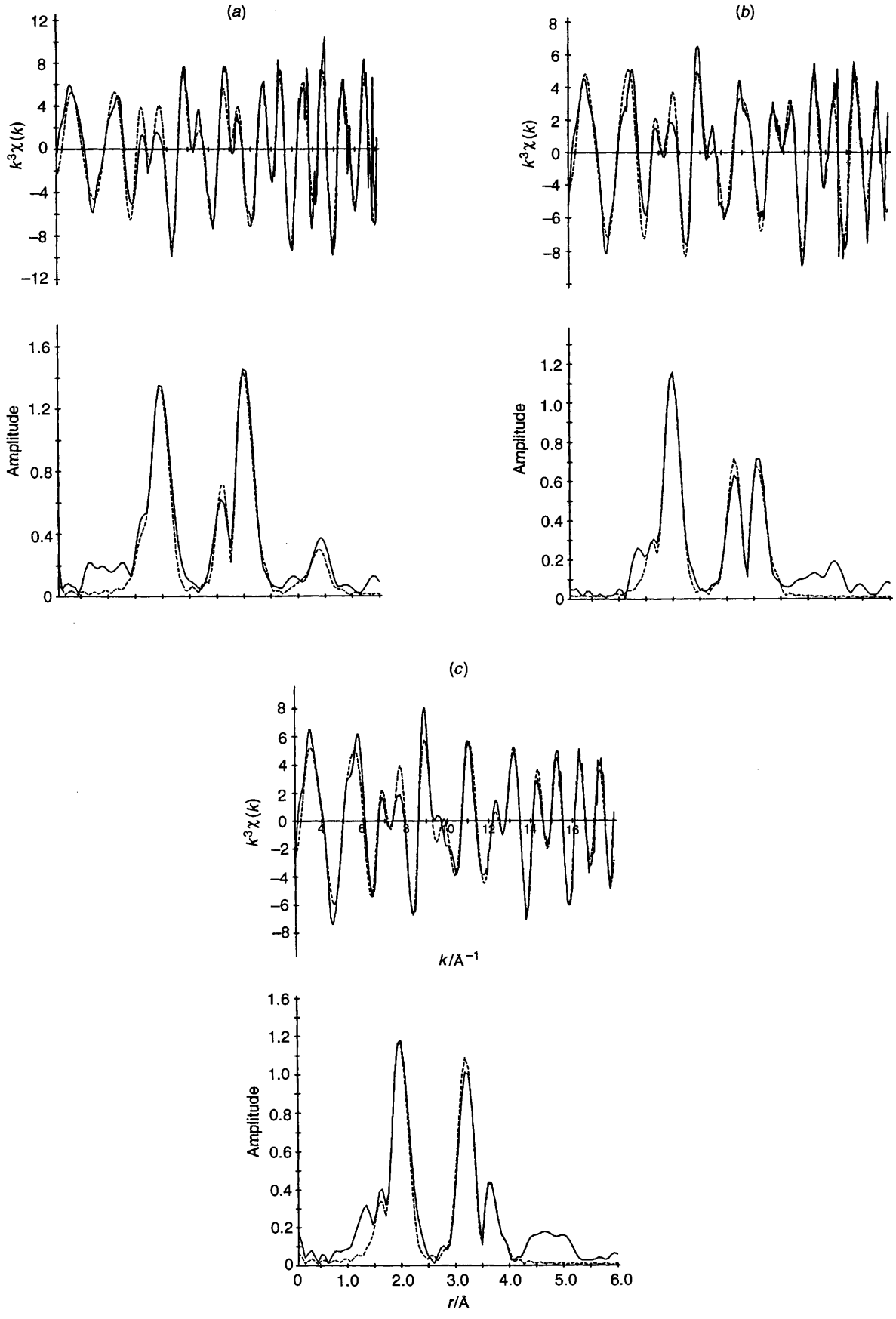

Fig. 4 Low-temperature (80 K) solid-state niobium K-edge k^3-weighted EXAFS data and Fourier transforms of $[NMe_4]Na_2K[Nb_2W_4O_{19}]$ (*a*), $[NMe_4]Na_2K_2[Nb_3W_3O_{19}]$ (*b*) and $Na_4K_2[Nb_4W_2O_{19}]$ (*c*). Details as in Fig. 2

(absorbing element in bold type). Given that $[Nb_2W_4O_{19}]^{4-}$ and $[Nb_4W_2O_{19}]^{6-}$ (abbreviated Nb_xW_{6-x}) are both *cis* isomers, the long **W**···M and **Nb**···M shells respectively should comprise contributions from both tungsten and niobium (co-ordination number = 0.5 each). However, acceptable results could only be obtained if either one tungsten

Table 1 The EXAFS-derived structural parameters for hexametalates (single scattering calculations). Comparison with single-crystal X-ray distances

Anion[a]	Edge	Shell	Co-ordination number	r[b]/Å	$2\sigma^2$[c]/Å^2	r(crystal)[d]/Å	$E°$/eV	E_v[e]/eV	R(%)
$[HNb_6O_{19}]^{7-}$	Nb K	O	1.0	1.785(3)	0.0030(5)	1.77 (1.75–1.78)	26.1	−6.7	28.5
solid (80 K)		O	4.0	1.974(2)	0.0071(3)	2.01 (1.970–2.056)			
		Nb	4.0	3.323(1)	0.0073(1)	3.37 (3.316–3.431)			
		Nb	1.0	4.758(7)	0.0057(10)	4.76			
$[Mo_6O_{19}]^{2-}$	Mo K	O	1.0	1.667(3)	0.0007(3)	1.68 (1.667–1.680)	29.2	−5.5	31.0
solid (80 K)		O	4.0	1.871(4)	0.0159(10)	1.93 (1.904–1.943)			
		Mo	4.0	3.264(1)	0.0056(1)	3.28 (3.271–3.288)			
		Mo	1.0	4.657(5)	0.0030(6)	4.62			
solution[f]	Mo K	O	1.0	1.672(3)	0.0033(5)		29.5	−5.5	28.9
		O	4.0	1.874(4)	0.0178(9)				
		Mo	4.0	3.269(1)	0.0071(1)				
		Mo	1.0	4.666(6)	0.0055(8)				
$[Nb_2W_4O_{19}]^{4-}$	W L_{III}	O	1.0	1.720(6)	0.0044(9)		11.7	−8.0	45.1
solid (298 K)		O	4.0	1.914(4)	0.0092(6)				
		W	2.5	3.312(4)	0.0071(4)				
		Nb	1.5	3.334(6)	0.0072(11)				
solid (80 K)	W L_{III}	O	1.0	1.716(6)	0.0051(10)		11.2	−8.0	37.5
		O	4.0	1.907(4)	0.0090(6)				
		W	2.5	3.313(3)	0.0043(3)				
		Nb	1.5	3.335(5)	0.0041(8)				
	Nb K	O	1.0	1.741(4)	0.0030(7)		25.6	−4.5	31.2
		O	4.0	1.994(3)	0.0077(5)				
		W	2.8	3.320(2)	0.0049(3)				
		Nb	1.2	3.350(5)	0.0039(9)				
		W	1.0	4.737(5)	0.0039(9)				
$[Nb_3W_3O_{19}]^{5-}$	W L_{III}	O	1.0	1.743(5)	0.0042(7)		11.6	−7.5	35.3
solid (80 K)		O	4.0	1.910(3)	0.0062(3)				
		W	2.0	3.295(3)	0.0048(4)				
		Nb	2.0	3.316(3)	0.0024(4)				
		Nb	1.0	4.780(7)	0.0049(9)				
	Nb K	O	1.0	1.763(4)	0.0045(6)		24.3	−5.5	30.2
		O	4.0	1.988(2)	0.0082(4)				
		W	2.0	3.327(3)	0.0059(2)				
		Nb	2.0	3.337(3)	0.0090(5)				
$[Nb_4W_2O_{19}]^{6-}$	W L_{III}	O	1.0	1.720(4)	0.0014(5)		14.4	−7.0	33.4
solid (80 K)		O	4.0	1.891(3)	0.0058(3)				
		W	1.0	3.295(8)	0.0064(10)				
		Nb	3.0	3.310(3)	0.0051(4)				
		Nb	1.0	4.735(6)	0.0032(7)				
	Nb K	O	1.0	1.756(3)	0.0036(5)		25.8	−4.8	25.3
		O	4.0	1.979(2)	0.0085(3)				
		W	1.5	3.338(2)	0.0052(2)				
		Nb	2.5	3.329(2)	0.0083(3)				
$[VW_5O_{19}]^{3-}$	W L_{III}	O	1.0	1.720(4)	0.0030(7)		12.5	−4.0	26.0
solid (298 K)		O	3.0	1.910(3)	0.0090(4)				
		W	3.0	3.270(2)	0.0080(2)				
		W	1.0	4.660(6)	0.0060(8)				
$[V_2W_4O_{19}]^{4-}$	W L_{III}	O	1.0	1.743(6)	0.0049(9)	1.70 (1.60–1.82)	12.5	−4.0	26.0
solid (80 K)		O	4.0	1.919(4)	0.0094(6)	1.94 (1.77–2.09)			
		W	2.5	3.272(2)	0.0044(1)	3.27 (3.168–3.347)			
		V	1.5	3.197(5)	0.0049(8)	3.27 (3.168–3.347)			
	V K	O	4.0	1.910(11)	0.0116(19)		10.0	−4.5	76.1
		W	3.0	3.217(9)	0.0066(11)				

[a] See experimental for counter ions. [b] Standard deviations in parentheses. [c] Debye–Waller factor; σ = root-mean-square internuclear separation. [d] $[HNb_6O_{19}]^{7-}$, X-ray data from ref. 13 for $Na_7[H_3O][Nb_6O_{19}]\cdot 14H_2O$; $[Mo_6O_{19}]^{2-}$, X-ray data from ref. 10 for $[NBu^n_4]_2[Mo_6O_{19}]$; $[V_2W_4O_{19}]^{4-}$, averaged values of W–O an V–O or W ··· W, W ··· V and V ··· V distances from crystal structure of α-$[CN_3H_6]_4[V_2W_4O_{19}]$.[14] [e] Virtual potential representing inelastic losses and core-hole lifetime effects. [f] Saturated solution of tetra-*n*-butylammonium salt in acetonitrile.

or one niobium atom was fitted in addition to the four shells shown in Table 1.* Fair improvements in the fits to the niobium K-edge EXAFS of Nb_2W_4 and tungsten L_{III}-edge EXAFS of Nb_4W_2 were obtained on addition of a sixth shell of one OM_6 oxygen. For the former: R = 30.5%, r = 2.347(2) Å and $2\sigma^2$ = 0.0103(38) Å^2 (99% probability of being significant). For the latter: R = 32.6%, r = 2.279(20) Å and $2\sigma^2$ = 0.0128(47) Å^2 (95% probability of being significant).

* For Nb_2W_4 and M = W: R = 36.4%, r = 4.656(8) Å and $2\sigma^2$ = 0.0061(10) Å^2. For Nb_2W_4 and M = Nb: R = 36.2%, r = 4.784(8) Å and $2\sigma^2$ = 0.0047(12) Å^2. For Nb_4W_2 and M = W: R = 25.0%, r = 4.645(16) Å and $2\sigma^2$ = 0.0139(25) Å^2. For Nb_4W_2 and M = Nb: R = 24.4%, r = 4.767(10) Å and $2\sigma^2$ = 0.0108(16) Å^2.

Decametalates

The structures of $[W_{10}O_{32}]^{4-}$ and $[V_{10}O_{28}]^{6-}$ are related to that of the hexametalate-type ion (Fig. 1). In $[W_{10}O_{32}]^{4-}$ two W_5O_{18} units (defect W_6O_{19} units) are bonded mirror-symmetrically through four corner-sharing oxygen atoms with the formation of an octahedral space. In $[V_{10}O_{28}]^{6-}$ ten VO_6 octahedra share edges to form a structure with approximate D_{2h}

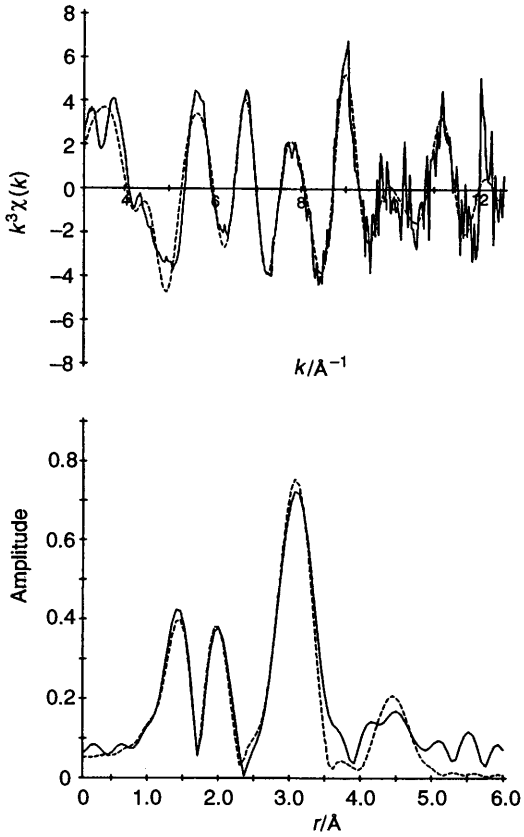

Fig. 5 Vanadium K-edge k^3-weighted EXAFS data and Fourier transform of $[NH_4]_6[V_{10}O_{28}]$ in the solid state at 80 K. Details as in Fig. 2

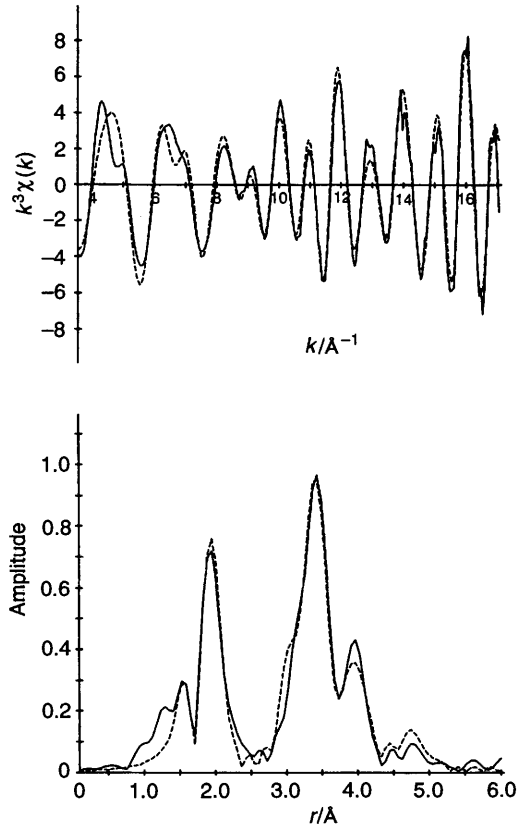

Fig. 6 Tungsten L_{III}-edge k^3-weighted EXAFS data and Fourier transform of $[NBu^n_4]_4[W_{10}O_{32}]$ in the solid state at 25 °C. Details as in Fig. 2

symmetry that resembles two octahedral V_6O_{19} units joined to share one V · · · V edge.

$[V_{10}O_{28}]^{6-}$. Evans[11] carried out an X-ray study of the decavanadate ion in crystals of $K_2Zn_2V_{10}O_{28}\cdot 16H_2O$ and these data have been used to generate a model to fit the low-temperature vanadium K-edge EXAFS of $[NH_4]_6[V_{10}O_{28}]$ in the solid state (Fig. 5, Table 2). There are three distinct vanadium sites in the ideal structure (orthorhombic molecular symmetry): V_I, V_{II} (vanadium displaced toward one apex of the VO_6 octahedron) and V_{III} (vanadium displaced toward one edge).* The EXAFS was only analysable up to *ca.* $k = 12.5$ Å^{-1} but despite this a good theoretical fit was obtained with a six-shell model. The two V–O shells expected at about 1.61 Å (one O_t) and 1.70 Å (short O_b, co-ordination number = 0.4) could not be resolved and only one shell was fitted at 1.62 Å. As a result, the Debye–Waller parameter for this shell is rather high for such a short distance. The V–O_b shell at 1.87 Å is also poorly defined ($2\sigma^2 = 0.036$ Å^2) and this is probably due to a large spread in bond lengths (1.803–2.077 Å for $K_2Zn_2V_{10}O_{28}\cdot 16H_2O$).

$[W_{10}O_{32}]^{4-}$. The best fit to the room-temperature tungsten L_{III}-edge EXAFS of $[NBu^n_4]_4[W_{10}O_{32}]$ in the solid state was achieved with three W · · · W shells and two shells for terminal and doubly bridging oxygen (Fig. 6, Table 2). The EXAFS-derived short and long W · · · W distances of 3.27 Å and 4.65 Å are in close agreement with the mean crystallographic values determined by Fuchs *et al.*[12] in the $[NBu^n_3H]^+$ salt. In between these two shells is a W · · · W separation at 3.86 Å which comes from the almost linear (175°) W–O–W bridges that link the two halves of the anion.

* Each V_I or V_{II} atom is bonded to one OV terminal oxygen (1.602–1.608 Å) and one OV_6 six-fold bridging oxygen (2.218–2.355 Å). In addition, each V_{II} atom is bonded to four OV_2 oxygens (1.837–1.907 Å) and each V_I atom to two OV_3 oxygens (1.965–2.014 Å). The V_{III} atoms are each bonded to two OV_2 oxygens (1.678–1.713 Å), two OV_3 oxygens (1.917–1.945 Å) and two OV_6 oxygens (2.110–2.123 Å). Apart from the V_{III} · · · V_{III} distance (3.31 Å), all of the V · · · V distances are in the range 3.052–3.187 Å.

Isopolymolybdates

The heptamolybdate anion is the predominant species formed on acidification of molybdate solutions to pH 3–5.5, $[MoO_4^{2-}] > 10^{-3}$ mol dm^{-3}. If, however, NBu^n_4Cl is added to such solutions the tetrabutylammonium salt of α-$[Mo_8O_{26}]^{4-}$ precipitates rather than that of $[Mo_7O_{24}]^{6-}$. If α-$[NBu^n_4]_4[Mo_8O_{26}]$ is dissolved in acetonitrile in the presence of potassium ions an isomerisation to β-$[Mo_8O_{26}]^{4-}$ takes place and β-$[NBu^n_4]_3K[Mo_8O_{26}]$ crystallises on cooling. The EXAFS models for the above three anions have been arrived at by examining the crystal structures of three salts: $Na_6[Mo_7O_{24}]\cdot 14H_2O$,[19] α-$[NBu^n_4]_4[Mo_8O_{26}]$[20] and β-$[NH_4]_4[Mo_8O_{26}]\cdot 4H_2O$.[21] Despite the complexity of the structures, the Mo–O bond lengths and non-bonded Mo · · · Mo distances may be grouped into a series of significant ranges (Table 2). The ions $[Mo_7O_{24}]^{6-}$ and β-$[Mo_8O_{26}]^{4-}$ are related in that both can be 'derived' from the $[V_{10}O_{28}]^{6-}$ structure by removal of three and two MO_6 octahedra respectively (Fig. 7). The α-$[Mo_8O_{26}]^{4-}$ anion consists of a ring made up of six MoO_6 octahedra linked to one MoO_4 tetrahedron above, and another below, its octahedral cavity.

Oxygen shells corresponding to short, medium and long Mo–O were fitted to the low-temperature molybdenum K-edge EXAFS of β-$[NBu^n_4]_3K[Mo_8O_{26}]\cdot H_2O$ (Fig. 8) and α-$[NBu^n_4]_4[Mo_8O_{26}]$ in the solid state (Table 2). Inclusion of a distant oxygen shell at 2.16 Å for $[NH_4]_6[Mo_7O_{24}]\cdot 4H_2O$ resulted in a significant decrease in the fit index from 0.67 to 0.60 but the shell was poorly defined ($2\sigma^2 = 0.032$ Å^2). For α-

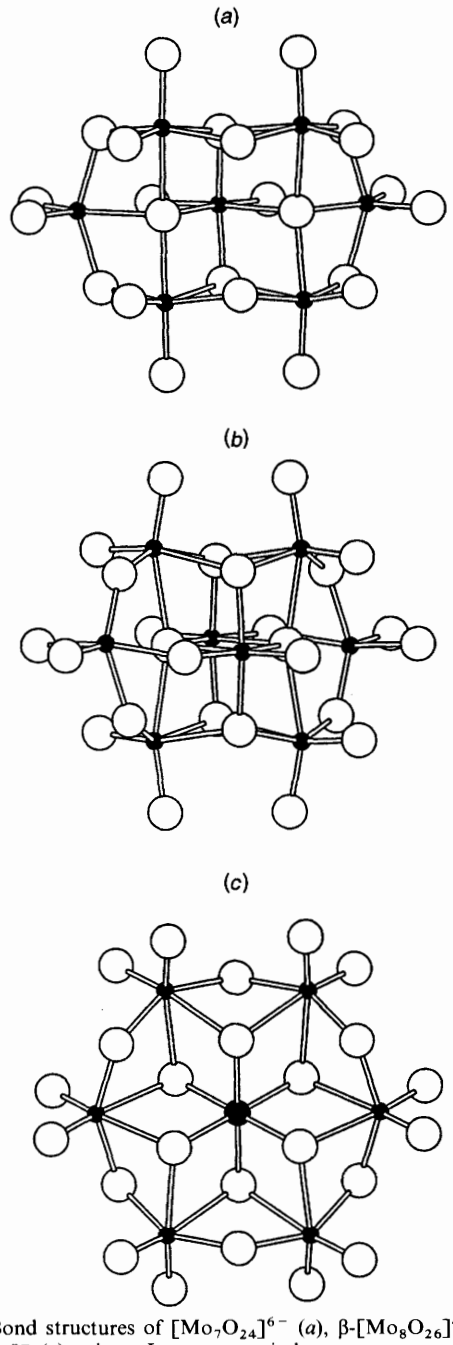

Fig. 7 Bond structures of $[Mo_7O_{24}]^{6-}$ (*a*), β-$[Mo_8O_{26}]^{4-}$ (*b*) and $MMo_6O_{24}^{n-}$ (*c*) anions. Large open circles represent oxygen atoms, small filled circles molybdenum atoms and the medium filled circle the heteroatom, M. Atomic coordinates from ref. 19 for $Na_6[Mo_7O_{24}]\cdot 14H_2O$, ref. 21 for β-$[NH_4]_4[Mo_8O_{26}]\cdot 4H_2O$ and ref. 22 for $Na_3[H_6CrMo_6O_{24}]\cdot 8H_2O$

$[Mo_8O_{26}]^{4-}$ it was not possible to resolve the two oxygen shells corresponding to *cis*-MoO_2 (crystallographic Mo–O_t 1.68 Å) and tetrahedral MoO_4 (crystallographic Mo–O 1.77 Å) units (average co-ordination numbers of 1.5 and 1.0 respectively). Instead, just one shell was fitted at 1.72 Å.

For $[Mo_7O_{24}]^{6-}$, Mo · · · Mo shells at 3.21 (co-ordination number = 0.8), 3.28 (0.6) and 3.42 Å (1.7) are predicted. In fact, only two shells at 3.20 and 3.38 Å could be fitted to the EXAFS (average co-ordination numbers of 1.4 and 1.7 respectively). For α-$[Mo_8O_{26}]^{4-}$, shells at 3.39 (co-ordination number = 1.5), 3.70 (0.25) and 3.82 (3.0) are predicted corresponding to Mo_{ring} · · · Mo_{ring}, Mo_{cap} · · · Mo_{cap} and Mo_{ring} · · · Mo_{cap} respectively. Only two shells at 3.33 and 3.73 Å could be fitted. The latter shell was poorly defined ($2\sigma^2$ = 0.03 $Å^2$), possibly due to a large spread in Mo_{ring} · · · Mo_{cap} distances and/or to the

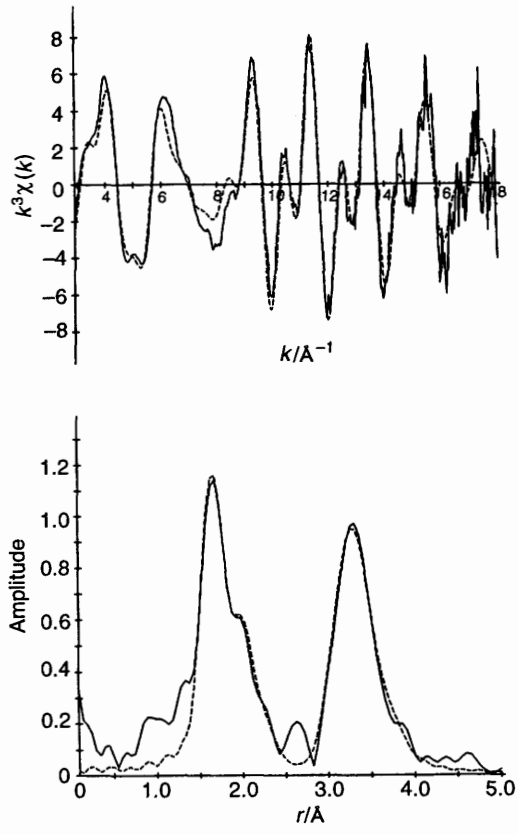

Fig. 8 Molybdenum K-edge k^3-weighted EXAFS data and Fourier transform of β-$[NBu^n_4]_3K[Mo_8O_{26}]\cdot H_2O$ in the solid state at 80 K. Details as in Fig. 2

proximity of a shell for Mo_{cap} · · · Mo_{cap}. For β-$[Mo_8O_{26}]^{4-}$ two shells at 3.24 (co-ordination number = 2.0) and 3.49 Å (2.3) are predicted and indeed the EXAFS was well fitted by two shells with distances close to these (3.22 and 3.43 Å).

Anderson ions of the type $MMo_6O_{24}^{n-}$

The Anderson[23] structure was first observed for $[TeMo_6O_{24}]^{6-}$ and has since been characterised in several heteropoly-tungstates and -molybdates [Fig. 7(*c*)]. The structure is analogous to that of α-$[Mo_8O_{26}]^{4-}$ in that it contains a ring of six edge-sharing MoO_6 octahedra. The central octahedral vacancy is occupied by a heteroatom in oxidation state 2–4, 6 or 7. Levason and co-workers[24] showed that a combination of iodine and metal-edge EXAFS could provide reliable structural data on Anderson polyanions of the type $M^1{}_n[H_{15-n}M^2{}_4I_3O_{24}]$ (M^2 = Co or Fe).

$[TeMo_6O_{24}]^{6-}$. Molybdenum K-edge X-ray absorption spectra were recorded for $Na_6[TeMo_6O_{24}]\cdot 2H_2O$ in the solid state at 80 K (Fig. 9) and also for a saturated solution of the salt in water. In both cases the k^3-weighted EXAFS was best fitted by a five-shell model of two OMo oxygens at 1.71 Å, two OMo_2 oxygens at 1.92 Å, two OMo_2Te oxygens at 2.25 Å, one tellurium at 3.23 Å and two molybdenum at 3.23 Å. The EXAFS-derived interatomic distances are compared in Table 3 with those found by Evans[25] in a single-crystal X-ray study of $[NH_4]_6[TeMo_6O_{24}]\cdot 7H_2O\cdot Te(OH)_6$. The Mo–O bond lengths are in good agreement but the EXAFS-derived Mo · · · Mo and Mo · · · Te distances are about 0.06 Å shorter.

Keggin ions of the type α-$[PM_{12}O_{40}]^{3-}$

For tungstates the α-Keggin[28] anion has approximate overall T_d symmetry and is based on a central XO_4 tetrahedron

Table 2 The EXAFS-derived structural parameters for isopolymetalates of the type $M_yO_z^{n-}$, $y > 6$. Comparison with single-crystal X-ray distances

Anion	Edge	Shell	Co-ordination number	r/Å	$2\sigma^2$/Å^2	r(crystal)[a]/Å	$E°$/eV	E_v/eV	R (%)
$[V_{10}O_{28}]^{6-}$ solid (80 K)	V K	O	1.2	1.617(5)	0.0101(10)	1.61 (1.602–1.608) 1.70 (1.678–1.713)	15.8	−2.0	32.4
		O	3.6	1.872(7)	0.0364(15)	1.91 (1.803–2.077)			
		V	4.8	3.095(6)	0.0226(9)	3.12 (3.052–3.187)			
		O	3.6	3.284(7)	0.0094(13)	3.41 (3.28–3.44)			
		O	1.2	2.228(9)	0.0123(22)	2.23 (2.110–2.355)			
		V	1.2	4.459(12)	0.0093(19)	4.44			
$[W_{10}O_{32}]^{4-}$ solid (298 K)	W L_{III}	O	1.0	1.722(4)	0.0035(6)	1.71 (1.68–1.76)	11.2	−7.3	27.0
		O	4.0	1.908(3)	0.0102(5)	1.93 (1.84–2.06)			
		W	3.2	3.272(2)	0.0077(2)	3.28 (3.251–3.298)			
		W	0.8	3.857(3)	0.0034(3)	3.79 (3.787–3.796)			
		W	0.8	4.651(7)	0.0061(10)	4.62 (4.615–4.621)			
$[Mo_7O_{24}]^{6-}$ solid (80 K)	Mo K	O	2.0	1.707(2)	0.0044(3)	1.72 (1.67–1.76)	31.5	−4.0	33.3
		O	2.0	1.908(5)	0.0131(11)	1.92 (1.88–2.01)			
		Mo	1.4	3.200(3)	0.0066(3)	3.21 (3.19–3.21) 3.28 (3.27–3.28)			
		Mo	1.7	3.383(3)	0.0085(5)	3.42 (3.41–3.45)			
α-$[Mo_8O_{26}]^{4-}$ solid (80 K)	Mo K	O	2.5	1.715(2)	0.0058(3)	1.68 (1.67–1.69) 1.77 (1.76–1.78)	28.7	−3.0	36.1
		O	1.5	1.905(3)	0.0036(4)	1.90 (1.88–1.92)			
		O	1.5	2.350(10)	0.0161(27)	2.44 (2.35–2.53)			
		Mo	1.5	3.328(5)	0.0147(9)	3.39 (3.38–3.41)			
		Mo	3.0	3.728(12)	0.0298(27)	3.70[b] 3.82 (3.77–3.88)			
β-$[Mo_8O_{26}]^{4-}$ solid (80 K)	Mo K	O	2.0	1.701(2)	0.0036(2)	1.71 (1.69–1.72)	28.9	−2.0	31.1
		O	2.0	1.927(3)	0.0074(6)	1.94 (1.85–2.01)			
		O	2.0	2.280(9)	0.0225(29)	2.33 (2.18–2.48)			
		Mo	2.0	3.223(2)	0.0096(4)	3.24 (3.22–3.26)			
		Mo	2.3	3.434(3)	0.0115(5)	3.49 (3.43–3.58)			

[a] $[V_{10}O_{28}]^{6-}$, X-ray data from ref. 11 for $K_2Zn_2[V_{10}O_{28}]\cdot16H_2O$, interatomic distances averaged over ideal orthorhombic symmetry; $[W_{10}O_{32}]^{4-}$, X-ray data from ref. 12 for $[NBu^n_3H]_4[W_{10}O_{32}]$; $[Mo_7O_{24}]^{6-}$, X-ray data from ref. 19 for $Na_6[Mo_7O_{24}]\cdot14H_2O$; α-$[Mo_8O_{26}]^{4-}$, X-ray data from ref. 20 for α-$[NBu^n_4]_4[Mo_8O_{26}]$; β-$[Mo_8O_{26}]^{4-}$, X-ray data from ref. 21 for β-$[NH_4]_4[Mo_8O_{26}]\cdot4H_2O$. [b] Separation of tetrahedrally co-ordinated molybdenum capping atoms.

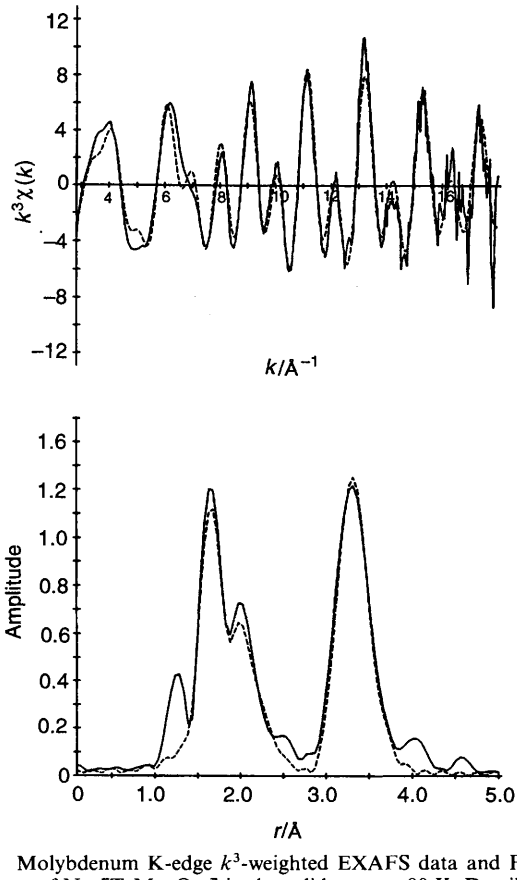

Fig. 9 Molybdenum K-edge k^3-weighted EXAFS data and Fourier transform of $Na_6[TeMo_6O_{24}]$ in the solid state at 80 K. Details as in Fig. 2

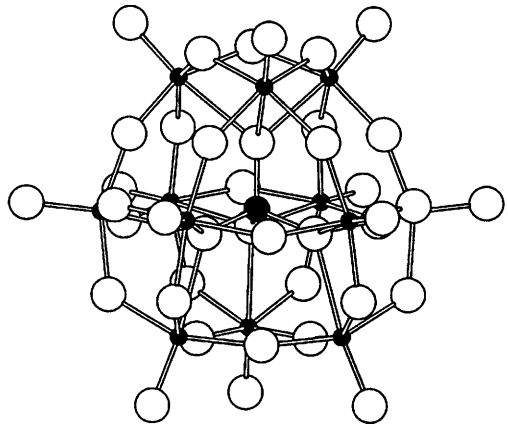

Fig. 10 Bond structure of the α-$[XM_{12}O_{40}]^{n-}$ anion. Large open circles represent oxygen atoms, small filled circles M atoms and the medium filled circle the X atom. Atomic coordinates from ref. 27 for α-$[H_5O_2]_3[PW_{12}O_{40}]$

surrounded by twelve MO_6 octahedra arranged in four groups of three edge-shared octahedra, M_3O_{13} (Fig. 10).[26] These groups are linked by sharing corners to each other and to the central XO_4 tetrahedron. In contrast, the corresponding molybdates adopt a structure in which all the mirror planes have been lost as a result of displacement of the molybdenum atoms within their MoO_6 octahedra.[27] All *trans*-related O–Mo–O–Mo bonds alternate in length and the overall structure is chiral (point group *T*).

α-$[PW_{12}O_{40}]^{3-}$. The simplest fit to the room-temperature tungsten L_{III}-edge EXAFS of $[NBu^n_4]_3[PW_{12}O_{40}]$ in the solid

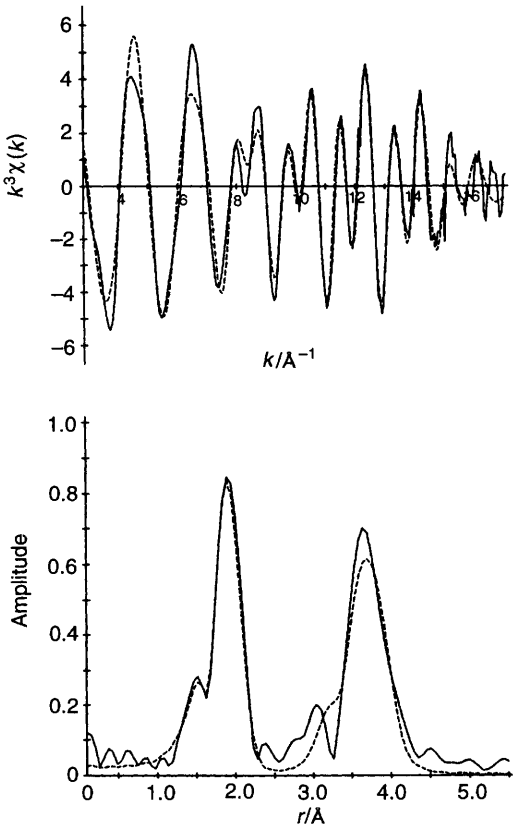

Fig. 11 Tungsten L_{III}-edge k^3-weighted EXAFS data and Fourier transform of α-$[NBu^n_4]_3[PW_{12}O_{40}]$ in the solid state at 25 °C. Details as in Fig. 2

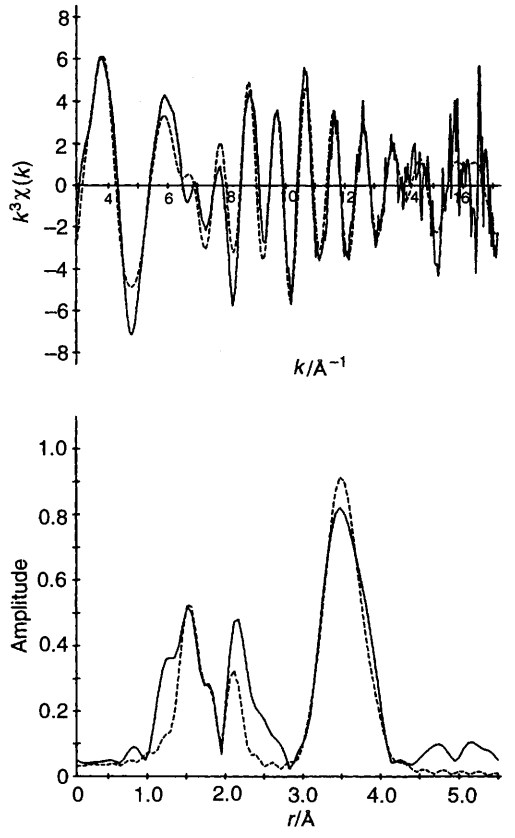

Fig. 12 Molybdenum K-edge k^3-weighted EXAFS data and Fourier transform of α-$[NBu^n_4]_3[PMo_{12}O_{40}]$ in the solid state at 80 K. Details as in Fig. 2

state was achieved with one OW terminal oxygen at 1.71 Å, four OW_2 doubly bridged oxygens at 1.90 Å, two tungstens at 3.40 Å corresponding to edge-sharing WO_6 octahedra and two tungstens at 3.68 Å corresponding to corner-sharing WO_6 octahedra (Fig. 11, Table 3). These results are in good agreement with the crystallographic data for dodecatungstophosphoric acid hexahydrate.[26] No OW_4 four-fold bridging oxygen shell, expected at *ca.* 2.43 Å, could be included in the model. A statistically valid shell of 1.3 phosphorus atoms at 3.49 Å was subsequently fitted to the EXAFS. This brought F and R from 0.51 and 28.8% to 0.47 and 25.8% respectively. However, the refined distance is about 0.06 Å shorter than expected. Also the shell had to be fitted with a co-ordination number of 1.3 since if only one phosphorus was fitted then $2\sigma^2$ for the shell refined to a very low value (< 0.001 Å^2).

α-$[PMo_{12}O_{40}]^{3-}$. Miyanaga *et al.*[8] carried out EXAFS experiments on various polyoxo-molybdate and -tungstate compounds and reported that the OMo_2 oxygen peaks which should appear at *ca.* 1.9 Å in the Fourier transforms of the EXAFS for $[Mo_6O_{19}]^{2-}$ and $[PMo_{12}O_{40}]^{3-}$ were hardly discernible, while the tungstates and other molybdates gave the metal–oxygen peaks normally. As noted above, they concluded that the Debye–Waller factors for the metal-bridging oxygen bonds in the two anions are exceptionally large ($\sigma \geqslant 0.08$ Å). While this is probably true for hexamolybdate, the authors fail to consider that it could be the systematic asymmetry in the Mo–O_b bonds in $[PMo_{12}O_{40}]^{3-}$ that results in peaks of diminished intensity in the Fourier transform.

The molybdenum K-edge EXAFS was analysed for $[NBu^n_4]_3[PMo_{12}O_{40}]$ in the solid state at 80 K (Fig. 12) and also for a saturated solution of the salt in acetonitrile. It soon became clear during curve-fitting analysis that the Mo–O_b distances were indeed resolved into two short and long components (Table 3). Thus the spectra were fitted by five-shell models that included shells of two OMo_2 oxygens at *ca.* 1.80 Å and two oxygens at *ca.* 1.95 Å. Not surprisingly, the two distances were highly correlated (*ca.* 0.8) but the fit-index contour maps of Mo–O_b (short) *versus* Mo–O_b (long) show reasonably well defined minima. Statistically valid shells of one OMo_4 oxygen atom were subsequently fitted to the EXAFS. For the solid-state spectrum this gave $R = 38.8\%$, $r = 2.390(11)$ Å and $2\sigma^2 = 0.0096(25)$ Å^2. For the solution spectrum a fit with $R = 32.5\%$, $r = 2.380(6)$ Å and $2\sigma^2 = 0.0079(13)$ Å^2 was obtained.

Conclusion

Polyoxometalates are best characterised in the solid state by X-ray diffraction but suitable crystals cannot always be grown and so there is still much scope for the development of new complementary methods such as fast atom bombardment mass spectrometry. We have obtained a wealth of structural information, much of it new, on various cluster ions by a combination of metal-edge EXAFS spectroscopy. These data have been shown to be reliable by comparison with X-ray crystallographic results, where available. Particular value arises with structures that are disordered crystallographically such as $[V_2W_4O_{19}]^{4-}$. It is clearly desirable to make use of as many independent experimental methods as possible in order to identify the solute species in polyanion solutions. Molybdenum K-edge EXAFS analysis data show that the framework structures of $[TeMo_6O_{24}]^{6-}$ and $[Mo_6O_{19}]^{2-}$ are not perturbed significantly after dissolving the salts $Na_6[TeMo_6O_{24}]\cdot nH_2O$ and $[NBu^n_4]_2[Mo_6O_{19}]$ in water and acetonitrile respectively. Direct structural evidence has also been found for the retention of the systematic asymmetry in the Mo–O_b bonds in $[NBu^n_4]_3[PMo_{12}O_{40}]$ when it is dissolved in acetonitrile.

Table 3 The EXAFS-derived structural parameters for heteropolymetalates. Comparison with single-crystal distances

Anion	Edge	Shell	Co-ordination number	r/Å	$2\sigma^2$/Å^2	r(crystal)[a]/Å	$E°$/eV	E_v/eV	R (%)
$[TeMo_6O_{24}]^{6-}$	Mo K	O	2.0	1.705(2)	0.0030(3)	1.71 (1.693–1.723)	29.4	−3.5	31.7
solid (80 K)		O	2.0	1.918(3)	0.0063(6)	1.94 (1.913–1.957)			
		O	2.0	2.251(8)	0.0151(22)	2.29 (2.282–2.316)			
		Te	1.0	3.227(3)	0.0036(3)	3.29 (3.282–3.300)			
		Mo	2.0	3.228(5)	0.0119(14)	3.29 (3.275–3.312)			
solution[b]	Mo K	O	2.0	1.713(1)	0.0034(2)		26.3	−3.5	24.1
		O	2.0	1.926(2)	0.0067(4)				
		O	2.0	2.255(6)	0.0191(18)				
		Te	1.0	3.231(3)	0.0055(3)				
		Mo	2.0	3.234(4)	0.0151(11)				
$[PW_{12}O_{40}]^{3-}$	W L_{III}	O	1.0	1.710(6)	0.0093(11)	1.70	13.8	−5.0	28.8
solid (298 K)		O	4.0	1.898(3)	0.0118(4)	1.90			
		W	2.0	3.403(3)	0.0105(4)	3.41			
		W	2.0	3.680(3)	0.0106(4)	3.70			
$[PMo_{12}O_{40}]^{3-}$	Mo K	O	1.0	1.670(4)	0.0028(6)	1.69 (1.64–1.70)	28.1	−3.0	41.9
solid (80 K)		O	2.0	1.809(5)	0.0054(6)	1.85 (1.83–1.89)			
		O	2.0	1.973(7)	0.0102(12)	1.96 (1.93–2.00)			
		Mo	2.0	3.411(3)	0.0096(4)	3.41			
		Mo	2.0	3.698(7)	0.0166(13)	3.70			
solution[c]	Mo K	O	1.0	1.656(3)	0.0030(5)		29.4	−3.0	37.3
		O	2.0	1.792(4)	0.0071(7)				
		O	2.0	1.939(6)	0.0117(12)				
		Mo	2.0	3.404(3)	0.0128(5)				
		Mo	2.0	3.687(5)	0.0163(10)				

[a] $[TeMo_6O_{24}]^{6-}$, X-ray data from ref. 25 for $[NH_4]_6[TeMo_6O_{24}]\cdot 2H_2O\cdot Te(OH)_6$; $[PW_{12}O_{40}]^{3-}$, neutron data from ref. 26 for α-$[H_5O_2]_3[PW_{12}O_{40}]$; $[PMo_{12}O_{40}]^{3-}$, X-ray data from ref. 27 for $H_3[PMo_{12}O_{40}]\cdot 13$–$14H_2O$. [b] Saturated solution of sodium salt in water. [c] Saturated solution of tetra-*n*-butylammonium salt in acetonitrile.

Experimental

Preparation of compounds

The following compounds were prepared and purified as reported previously: $[NBu^n_4]_2[Mo_6O_{19}]$,[2] $K_7[HNb_6O_{19}]$,[2] $[NBu^n_4]_3[VW_5O_{19}]$,[29] $Na_4[V_2W_4O_{19}]$,[29] $[NMe_4Na_2K[Nb_2W_4O_{19}]$,[30] $[NMe_4]Na_2K_2[Nb_3W_3O_{19}]$,[30] $Na_4K_2[Nb_4W_2O_{19}]$,[30] $[NH_4]_6[V_{10}O_{28}]$,[31] $[NBu^n_4]_4[W_{10}O_{32}]$,[32] α-$[NBu^n_4]_4[Mo_8O_{26}]$,[2] β-$[NBu^n_4]_3K[Mo_8O_{26}]$,[2] $[NBu^n_4]_3[PW_{12}O_{40}]$,[2] $[NBu^n_4]_3[PMo_{12}O_{40}]$[33] and $Na_6[TeMo_6O_{24}]$.[34] The compound $[NH_4]_6[Mo_7O_{24}]$ was obtained from May and Baker Ltd. and used without further purification. All samples were identified in the solid state by their IR spectra, which agreed with the spectra found previously for the same compounds[5,29,32,35] in all cases except that of the molybdate $[TeMo_6O_{24}]^{6-}$, for which no earlier spectrum was reported. The niobate complexes $Nb_xW_{6-x}O_{19}^{(x+2)-}$ were further characterised in solution by their UV spectra.[30]

EXAFS data acquisition and analysis

X-Ray absorption spectra were recorded in transmission mode on stations 7.1 [double crystal Si(111) order-sorting monochromator] and 9.2 [double crystal Si(220) order-sorting monochromator] of the Synchrotron Radiation Source at the Daresbury Laboratory, operating at 2 GeV (*ca.* 3.20×10^{-10} J) and an average current of 150 mA (range 117–270 mA). Solid samples were diluted if necessary with boron nitride and held between layers of sticky tape in 1 mm thick aluminium plates. For low-temperature measurements (*ca.* 80 K) the sample plates were mounted on either fixed or variable-temperature liquid-nitrogen cryostats. Aluminium cells of thickness 5 mm were used to obtain multiple solution spectra at room temperature. The personal computer resident program PAXAS[36] was used to extract the raw EXAFS, $\chi^E(k)$. Removal of the pre-edge background was achieved using a polynomial of order 2 and the post-edge background was subtracted by fitting this region with a polynomial of order 6, 7 or 8. Curve-fitting analyses, by least-squares refinement of the non-Fourier filtered k^3-weighted EXAFS data, were carried out within EXCURVE[37] (version EXCURV 92) on the Daresbury Convex C220, using spherical-wave methods with *ab initio* phase shifts and backscattering factors calculated in the usual manner from relativistic Hartree–Fock self-consistent field (HF-SCF) derived atomic charge densities. Statistically derived errors on the determined distances were generally below 0.01 Å but a more realistic estimate is 1.5%, or 0.02–0.07 Å for the distances quoted in this paper.[38] The statistical validity of shells was assessed by published means and, unless otherwise stated, the shells were found to have less than 1% probability of being insignificant.[17] The number of independent parameters used in the fits are within the guideline $N_{pts} = 2(k_{max} - k_{min})(R_{max} - R_{min})/\pi$.[39] The R factors are defined as $(\int|\chi^{calc} - \chi^{exptl}|k^3dk/\int|\chi^{exptl}|k^3dk) \times 100\%$ and the fit indexes as $\Sigma_i\{k_i{}^3[\chi_i{}^{calc}(k) - \chi_i{}^{exptl}(k)]\}^2$. Values of AFAC, the energy-independent parameter used to account for the reduction in EXAFS amplitude due to multiple excitations, were 0.95, 0.85, 0.90 and 0.90 for the niobium K-, molybdenum K-, tungsten L_{III}- and vanadium K-edge spectra respectively. Some of the molybdenum and niobium K-edge Fourier transforms contained features below 1 Å which could not be removed by variation in the background-subtraction procedure. However, these artifacts did not effect fitting of the real atomic shells.

Acknowledgements

We thank the SERC (M. P. and J. M. R) for support and the Director of the Daresbury Laboratory for the provision of facilities.

References

1 M. T. Pope, *Heteropolymetalates and Isopolymetalates*, Springer, Berlin, Heidelberg, 1983; V. W. Day and W. G. Klemperer, *Science*, 1985, **228**, 533; M. T. Pope and A. Müller, *Angew. Chem., Int. Ed. Engl.*, 1991, **30**, 34.

2 M. Filowitz, R. K. C. Ho, W. G. Klemperer and W. Shum, *Inorg. Chem.*, 1979, **18**, 93.

3 S. E. O'Donnell and M. T. Pope, *J. Chem. Soc., Dalton Trans.*, 1976, 2290; R. Acerete, C. F. Hammer and L. C. W. Baker, *J. Am. Chem. Soc.*, 1982, **104**, 5384; O. W. Howarth, P. Kelly and L. Pettersson, *J. Chem. Soc., Dalton Trans.*, 1990, 81; J. J. Hastings and O. W. Howarth, *J. Chem. Soc., Dalton Trans.*, 1992, 209.
4 L. Pettersson, I. Andersson and L.-O. Öhman, *Inorg. Chem.*, 1986, **25**, 4726.
5 C. Rocchiccioli-Deltcheff, R. Thouvenot and M. Dabbabi, *Spectrochim. Acta, Part A*, 1977, **33**, 143.
6 J. Evans, M. Pillinger and J.-J. Zhang, following paper.
7 J. M. Corker, J. Evans and J. M. Rummey, *Mater. Chem. Phys.*, 1991, **29**, 201; K. Bornholdt, J. M. Corker, J. Evans and J. M. Rummey, *Inorg. Chem.*, 1991, **30**, 1; J. F. W. Mosselmans, J. M. Corker, J. Evans, J. T. Gauntlett and J. M. Rummey, *Catal. Today*, 1991, **9**, 175.
8 T. Miyanaga, N. Matsubayashi, T. Fukumoto, K. Yokoi, I. Watanabe, K. Murata and S. Ikeda, *Chem. Lett.*, 1988, 487; T. Miyanaga, T. Fujikawa, N. Matsubayashi, T. Fukumoto, K. Yokoi, I. Watanabe and S. Ikeda, *Bull. Chem. Soc. Jpn.*, 1989, **62**, 1791.
9 I. Lindqvist, *Ark. Kemi*, 1953, **5**, 247.
10 P. Dahlstrom, J. Zubieta, B. Neaves and J. R. Dilworth, *Cryst. Struct. Commun.*, 1982, **11**, 463.
11 H. T. Evans, *Inorg. Chem.*, 1966, **5**, 967.
12 J. Fuchs, H. Hartl, W. Schiller and U. Gerlach, *Acta Crystallogr., Sect. B*, 1976, **32**, 740.
13 A. Goiffon, E. Philippot and M. Maurin, *Rev. Chim. Miner.*, 1980, **17**, 466.
14 K. Nishikawa, A. Kobayashi and Y. Sasaki, *Bull. Chem. Soc. Jpn.*, 1975, **48**, 889.
15 B.-K. Teo, *J. Am. Chem. Soc.*, 1981, **103**, 3990.
16 J. Fuchs, W. Freiwald and H. Hartl, *Acta Crystallogr., Sect. B*, 1978, **34**, 1764.
17 R. W. Joyner, K. J. Martin and P. Meehan, *J. Phys. C*, 1987, **20**, 4005.
18 H. K. Shae, W. G. Klemperer and V. W. Day, *Inorg. Chem.*, 1989, **28**, 1423.
19 K. Sjöbom and B. Hedman, *Acta Chem. Scand., Ser. A*, 1973, **27**, 3673.
20 J. Fuchs and H. Hartl, *Angew. Chem., Int. Ed. Engl.*, 1976, **15**, 375.
21 H. Vivier, J. Bernard and H. Djomaa, *Rev. Chim. Miner.*, 1977, **14**, 584.
22 A. Perloff, *Inorg. Chem.*, 1970, **9**, 2228.
23 J. S. Anderson, *Nature (London)*, 1937, **140**, 850.
24 R. D. Oldroyd, W. Levason and M. Webster, *J. Chem. Soc., Dalton Trans.*, 1994, 2983; E. M. Jones, W. Levason, R. D. Oldroyd, M. Webster, M. Thomas and J. Hutchings, *J. Chem. Soc., Dalton Trans.*, 1995, 3367.
25 H. T. Evans, *Acta Crystallogr., Sect. B*, 1974, **30**, 2095.
26 G. M. Brown, M.-R. Noe-Spirlet, W. R. Busing and H. A. Levy, *Acta Crystallogr., Sect. B*, 1977, **33**, 1038.
27 H. D'Amour and R. Allmann, *Z. Kristallogr.*, 1976, **143**, 1.
28 J. F. Keggin, *Nature (London)*, 1933, **131**, 908; *Proc. R. Soc. London, Ser. A*, 1934, **144**, 75.
29 C. M. Flynn and M. T. Pope, *Inorg. Chem.*, 1971, **10**, 2524.
30 M. Dabbabi and M. Boyer, *J. Inorg. Nucl. Chem.*, 1976, **38**, 1011.
31 G. K. Johnson and R. K. Murmann, *Inorg. Synth.*, 1979, **19**, 140.
32 A. Chemseddine, C. Sanchez, J. Livage, J. P. Launay and M. Fournier, *Inorg. Chem.*, 1984, **23**, 2609.
33 C. Sanchez, J. Livage, J. P. Launay, M. Fournier and Y. Jeannin, *J. Am. Chem. Soc.*, 1982, **104**, 3194.
34 S. R. Wood and A. Carlson, *J. Am. Chem. Soc.*, 1939, **61**, 1810.
35 C. Rocchiccioli-Deltcheff, R. Thouvenot and M. Fouassier, *Inorg. Chem.*, 1982, **21**, 30; J. Fuchs, S. Mahjour and R. Palm, *Z. Naturforsch., Teil B*, 1976, **31**, 544; W. G. Klemperer and W. Shum, *J. Am. Chem. Soc.*, 1976, **98**, 8291; C. Rocchiccioli-Deltcheff, M. Fournier, R. Franck and R. Thouvenot, *Inorg. Chem.*, 1983, **22**, 207.
36 N. Binsted, PAXAS Program for the analysis of X-ray absorption spectra, University of Southampton, 1988.
37 S. J. Gurman, N. Binsted and I. Ross, *J. Phys. C*, 1984, **17**, 143; 1986, **19**, 1845.
38 B. K. Teo, *EXAFS: Basic Principles and Data Analysis*, Springer, Berlin, 1986; S. J. Gurman, in *Applications of Synchrotron Radiation*, eds. C. R. A. Catlow and G. N. Greaves, Blackie, Glasgow, 1989.
39 F. W. Lytle, D. E. Sayers and E. A. Stern, *Physica B + C (Amsterdam)*, 1989, **158**, 701.

Received 11*th January* 1996; *Paper* 6/00220J